iScience

Article

Adenine base editing with engineered virus-like particles rescues the *CFTR* mutation G542X in patient-derived intestinal organoids

Graphical abstract

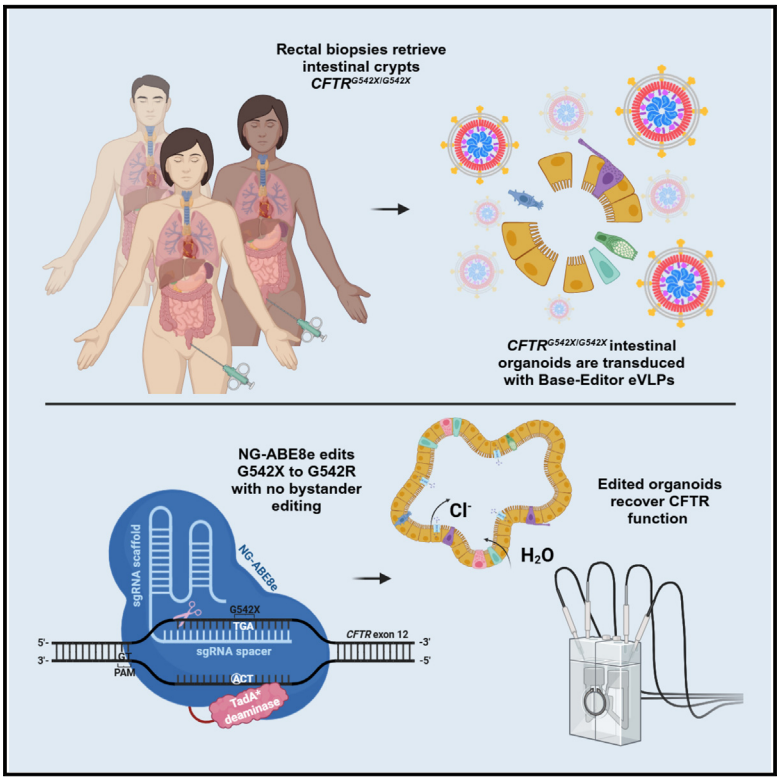

Highlights

- BE-eVLPs successfully deliver NG-ABE8e/sgRNA RNPs in patient-derived intestinal organoids
- NG-ABE8e edits G542X to G542R with no bystander and no off-target effect
- ~2% G542X-to-G542R editing efficiency restores ~6.4% of WT CFTR activity

Authors

Lucia Nicosia, Iwona Pranke, Roberta V. Latorre, ..., Isabelle Sermet-Gaudelus, Martina F. Scallan, Patrick T. Harrison

Correspondence

patrick.harrison@cchmc.org

In brief

Health sciences; Clinical genetics; Cellular therapy; Genetic engineering

Nicosia et al., 2025, iScience *28*, 111979
March 21, 2025
https://doi.org/10.1016/j.isci.2025.111979

CellPress

iScience

CellPress
OPEN ACCESS

Article

Adenine base editing with engineered virus-like particles rescues the *CFTR* mutation G542X in patient-derived intestinal organoids

Lucia Nicosia,[1,2] Iwona Pranke,[3,4,10] Roberta V. Latorre,[5,10] Joss B. Murray,[1] Lisa Lonetti,[1] Kader Cavusoglu-Doran,[1] Elise Dreano,[3,4] James P. Costello,[2] Michael Carroll,[2] Paola Melotti,[6] Claudio Sorio,[5] Isabelle Sermet-Gaudelus,[3,4,7,8] Martina F. Scallan,[2,11] and Patrick T. Harrison[1,9,11,12,*]

[1]Department of Physiology, University College Cork, Cork, Ireland
[2]School of Microbiology, University College Cork, Cork, Ireland
[3]INSERM, CNRS, Institut Necker Enfants Malades, Paris, France
[4]Université Paris-Cité, Paris, France
[5]Department of Medicine, University of Verona, Verona, Italy
[6]Cystic Fibrosis Center, Azienda Ospedaliera Universitaria Integrata Verona, Verona, Italy
[7]Cystic Fibrosis National Pediatric Reference Center, Pneumo-Allergologie Pédiatrique, Hôpital Necker Enfants Malades, , Assistance Publique Hôpitaux de Paris (AP-HP), Paris, France
[8]European Reference Network, ERN-Lung CF, Frankfurt am Mein, Germany
[9]Division of Pulmonary Medicine, Cincinnati Children's Hospital, Cincinnati, OH, USA
[10]These authors contributed equally
[11]These authors contributed equally
[12]Lead contact
*Correspondence: patrick.harrison@cchmc.org
https://doi.org/10.1016/j.isci.2025.111979

SUMMARY

Cystic fibrosis (CF) is a life-shortening autosomal recessive disease, caused by loss-of-function mutations that affect the CF transmembrane conductance regulator (CFTR) anion channel. G542X is the second-most common CF-causing variant, and it does not respond to current CFTR modulator drugs. Our study explores the use of adenine base editing to edit G542X to a non-CF-causing variant, G542R, and recover CFTR function. Using base editor engineered virus-like particles (BE-eVLPs) in patient-derived intestinal organoids, we achieved ~2% G542X-to-G542R editing efficiency and restored CFTR-mediated chloride transport to ~6.4% of wild-type levels, independent of modulator treatment, and with no bystander edits. This proof-of-principle study demonstrates the potential of base editing to rescue G542X and provides a foundation for future *in-vivo* applications.

INTRODUCTION

Approximately 162,000 people, across 94 countries, are estimated to be living with cystic fibrosis (CF), a life-shortening autosomal recessive disease.[1] CF is caused by loss-of-function mutations in the CF transmembrane conductance regulator (*CFTR*) gene that alter the synthesis, folding, trafficking, and/or gating properties of the CFTR anion channel, which mediates Cl^- and HCO^-_3 ion transport.[2,3] Modulator drugs, known as correctors and potentiators, have been developed that can restore function to many, but not all, CFTR protein variants.[4–10] Our study focuses on the second most common CF-causing mutation, c.1624G>T (www.genet.sickkids.on.ca, www.CFTR2.org), which generates a TGA premature termination codon (PTC) commonly known as G542X. This PTC triggers nonsense-mediated mRNA decay (NMD)[11,12] and renders the G542X variant unresponsive to modulator treatment.

Several proof-of-principle studies on *CFTR* gene editing have been published that reported restoration of CFTR expression and activity by homology-directed repair (HDR),[13] non-homologous end joining (NHEJ),[14] base editing,[15] or prime editing.[16] While each editing strategy is associated with some level of undesired by-products, compared to other approaches, base editing is often desirable. It can generate precise single-nucleotide edits, and it does not involve double-strand breaks (DSBs) formation, which minimizes the risk of insertion/deletions (indels).[17] Base editing also does not require a large packaging capacity for delivery, and it is highly efficient in both replicating and fully differentiated cells.[17,18] Adenine base editing catalyzes the conversion of A-T to G-C base pairs[17,19,20] and can thus correct a PTC (TGA) into either a tryptophan (TGG) or an arginine (CGA). We and others have used adenine base editing to edit and restore the original codon and amino acid for other CF-causing mutations: c.3846G>A (W1282X) and c.1657C>T (R553X).[21,22] Here, we show how this technique can be applied to rescue

G542X, by converting it into a new variant: G542R. If adenine base editing was used to target the A of G542X stop codon, it would not restore the wild-type (WT) amino acid, glycine (G), at position 542; rather it could edit the TGA (stop, X) codon into TGG (tryptophan, W) which would generate G542W (Figure 1A). Alternatively, if targeted to the non-coding strand, adenine base editors (ABEs) could convert ACT to GCT to generate a CGA codon (arginine, R) in the coding strand and install G542R (Figure 1A). Of note, neither G542W nor G542R is listed as CF-causing (www.genet.sickkids.on.ca and www.CFTR2.org). Moreover, both have been identified as a product of PTC suppression for G542X,[23–26] which occurs when near-cognate aminoacyl-tRNAs accommodate an alternative amino acid at the PTC site into the nascent polypeptide.[24] Editing G542X into G542R seemed the most attractive proposition, as, in cell lines, the G542R variant has been shown to retain ~40%–70% of WT CFTR activity, that is ~2.5-fold higher than G542W functional rescue.[23,24,26] We tested this adenine base editing approach in intestinal organoids,[27] derived from rectal biopsies of three donors homozygous for G542X (*CFTR*$^{G542X/G542X}$), a commonly used model to develop and validate CFTR modulator drugs.

RESULTS

NG-ABE8e edits G542X to G542R with no bystander and no off-target effect in patient-derived intestinal organoids

Binding of an ABE to target DNA is mediated by a single-guide RNA (sgRNA), composed of a scaffold that forms a ribonucleoprotein (RNP) complex with the ABE, and a spacer that is complementary to the DNA fragment of interest (Figure 1B). Clamping of the RNP on target DNA also requires binding to a short protospacer adjacent motif (PAM) (Figure 1B).[17] To perform the editing of G542X to G542R, we selected NG-ABE8e,[20] an ABE that recognizes the NG PAM site available near the target ACT sequence on the opposite strand to codon 542 (Figure 1B). The sgRNA we designed places the target adenine at position 9, counting from the PAM-distal end of the protospacer (Figure 1C), which falls within the editing window of NG-ABE8e.[20] We further incorporated hybridization extended A-T inversion (HEAT) modifications in the sgRNA scaffold sequence (Figure 1C). HEAT changes have been previously shown to improve editing efficiency by (1) introducing a 5-bp extension in the hairpin (Figure 1C) and (2) swapping opposing bases of one T-A base pair in the TTTT motif of the stem (Figure 1C), which would otherwise act as a transcription termination signal downstream of the U6 promoter in the sgRNA plasmid.[28,29]

We initially tested our editing strategy in *CFTR*$^{G542X/G542X}$ intestinal organoids from two donors. For the delivery of the NG-ABE8e/sgRNA RNPs, we used base editor engineered virus-like particles (BE-eVLPs), a transient vector with potential for *in-vivo* translation.[30] We transduced single-cell suspensions of *CFTR*$^{G542X/G542X}$ intestinal organoids with BE-eVLPs carrying either NG-ABE8e and the G542X-specific sgRNA (G542X-BE-eVLPs), or NG-ABE8e only (sgRNA-less BE-eVLPs) as a negative control. We transduced the organoid-derived cells in suspension with an initial multiplicity of transduction (MOT) of ~60 BE-eVLPs/cell. Cells were then grown as two-dimensional (2D) intestinal organoids on filters for 21 days before DNA or RNA extraction; editing was assessed by high-throughput sequencing (HTS) and quantified with CRISPResso2.[31] While no DNA editing was observed in organoid-derived cells transduced with sgRNA-less BE-eVLPs (Figure 1D), we detected G542X-to-G542R editing in the total non-sorted population of organoid cells transduced with G542X-BE-eVLPs, with an average editing efficiency of ~2% (Figure 1D). We also analyzed the abundance of *CFTR* transcript carrying G542R in the organoid-derived cells transduced with G542X-BE-eVLPs and observed no detectable enrichment compared to DNA editing levels (Figure 1E).

To evaluate the frequency of editing by-products, we further investigated the abundance of bystander editing, indel formation, and off-target effects in the *CFTR*$^{G542X/G542X}$ intestinal organoids transduced with G542X-BE-eVLPs. Bystander editing occurs when base editors edit non-target nucleotides within the protospacer and install undesired mutations.[32] In the 20-nt long spacer binding region, we detected no editing above background levels at potential bystander sites (Figure 1F), which underscored the precision of the editing design. We also screened HTS reads for indel formation, albeit uncommon for base editing; no indels were detected by CRISPResso2 analysis (Figure S1). Finally, we interrogated off-target edits that are unintended modifications in the genome that can occur at non-target sites. The off-target effect is mostly sgRNA-dependent, as Cas9 can tolerate up to 3 mismatches between the sgRNA and the target locus.[33] To identify potential off-targets of the G542X sgRNA, we performed an *in-silico* analysis using CRISPOR[34] that found eight exonic off-targets with $\leq$3 mismatches (Figure 1G). Only one predicted off-target, located in the *ADAMTS6* locus, had three mismatches outside of the PAM-proximal seed sequence, which is considered the region with the most stringent sgRNA-binding dependency.[35] We amplified and sequenced the *ADAMTS6* predicted off-target site, and analysis with CRISPResso2 did not detect any off-target editing above background levels (Figure 1H). The remaining seven sites had one or more mismatches in the seed region, which decreases the likelihood of off-target editing.

G542R restores CFTR activity in patient-derived intestinal organoids

Previous studies in CF cell lines have shown that G542R successfully restores protein expression, which is entirely obliterated in a *CFTR*$^{G542X/G542X}$ background. Levels of protein maturation measured in Fisher Rat Thyroid (FRT) cells and Human Embryonic Kidney 293 (HEK 293) cells stably expressing G542R range widely between ~30% and ~90% of WT levels.[23,26] While we did not characterize the maturation of the newly generated CFTR protein variant in our model, we measured the restoration of CFTR function post transduction by short-circuit current (ΔIsc), across 2D layers of the intestinal organoids described in the previous section (Figure 2A).

Upon stabilization of baseline Isc, the epithelial Na^+ channel (ENaC) was inhibited with the ENaC blocker amiloride.[36] After activation of the transepithelial cAMP-dependent current by 3-isobutyl-1-methylxanthine and forskolin (Fsk), CFTR-dependent Cl^- transport was inhibited by the specific CFTR inhibitor

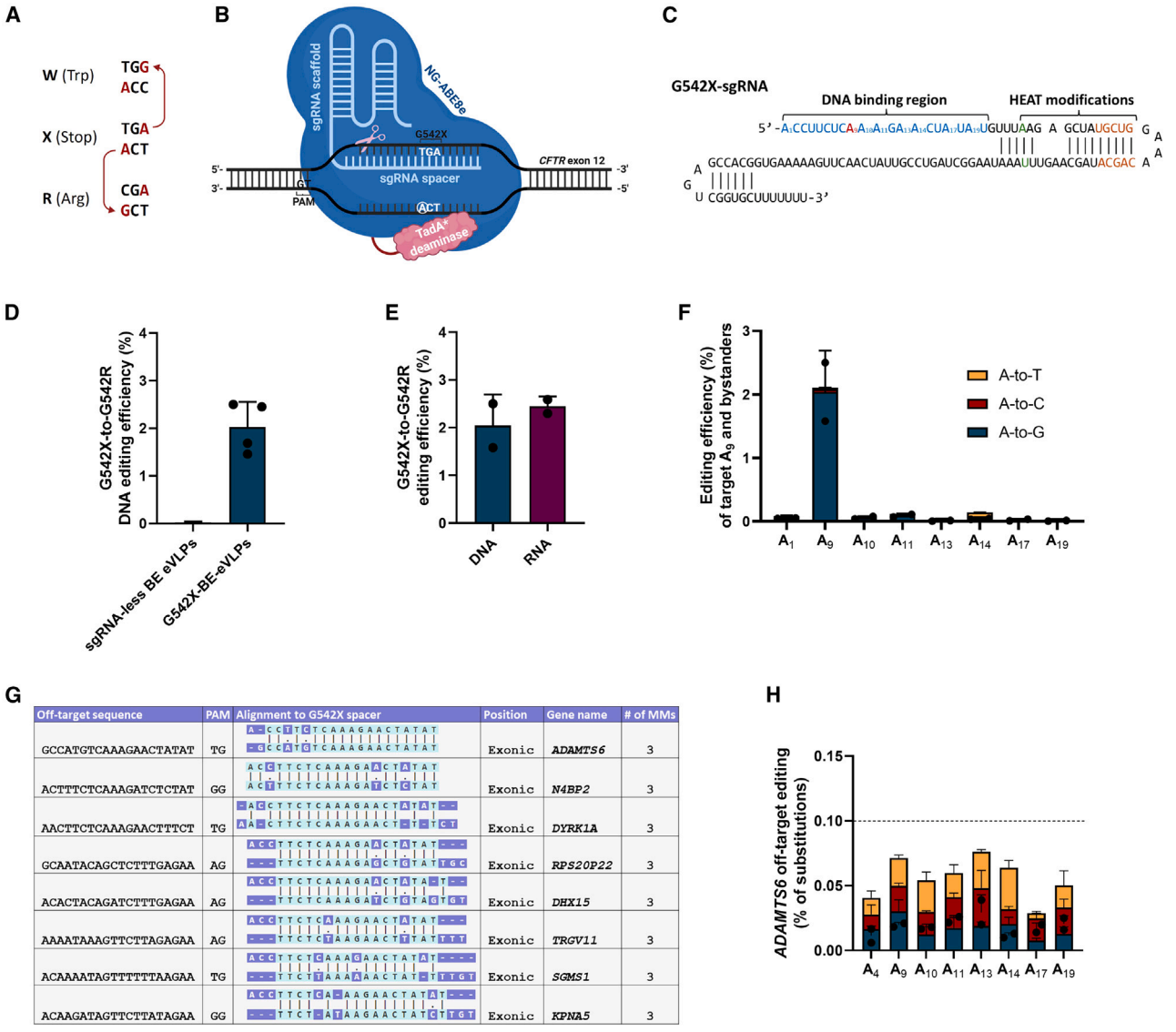

G

Off-target sequence	PAM	Alignment to G542X spacer	Position	Gene name	# of MMs
GCCATGTCAAAGAACTATAT	TG		Exonic	*ADAMTS6*	3
ACTTTCTCAAAGATCTCTAT	GG		Exonic	*N4BP2*	3
AACTTCTCAAAGAACTTTCT	TG		Exonic	*DYRK1A*	3
GCAATACAGCTCTTTGAGAA	AG		Exonic	*RPS20P22*	3
ACACTACAGATCTTTGAGAA	AG		Exonic	*DHX15*	3
AAAATAAAGTTCTTAGAGAA	AG		Exonic	*TRGV11*	3
ACAAAATAGTTTTTTAAGAA	TG		Exonic	*SGMS1*	3
ACAAGATAGTTCTTATAGAA	GG		Exonic	*KPNA5*	3

Figure 1. NG-ABE8e edits G542X to G542R with no bystander and no off-target effect in patient-derived intestinal organoids

(A) Schematic representation of possible outcomes of alternative adenine base editing approaches on G542X.

(B) The TadA* deoxyadenosine deaminase domain of NG-ABE8e deaminates the target deoxyadenosine (A, circled in white) to deoxyinosine in the non-coding strand of G542X on exon 12 of *CFTR*.

(C) Schematic representation of G542X sgRNA, including spacer (in blue), target adenine (in red), and scaffold with HEAT modifications (in green) in the stem and (in orange) in the hairpin.

(D) Editing efficiency quantified by amplicon sequencing of $CFTR^{G542X/G542X}$ intestinal organoid-derived cells transduced with sgRNA-less BE-eVLPs or G542X-BE-eVLPs (MOT = ∼60 G542X-BE-eVLPs/cell). Bars represent mean ± SD.

(E) Editing efficiency quantified by amplicon sequencing of DNA and RNA extracted from $CFTR^{G542X/G542X}$ intestinal organoid-derived cells transduced with G542X-BE-eVLPs (MOT = ∼60 G542X-BE-eVLPs/cell). Bars represent mean ± SD.

(F) Bystander editing analyzed by amplicon sequencing of $CFTR^{G542X/G542X}$ intestinal organoid-derived cells transduced with G542X-BE-eVLPs (MOT = ∼60 G542X-BE-eVLPs/cell). Bystander effect was quantified for each adenine around the target A_9 in the protospacer. Non-specific editing (A-to-T and A-to-C) was also quantified for each position. Bars represent mean ± SD.

(G) CRISPOR *in-silico* analysis of potential off-targets with ≤3 mismatches.

(H) Editing efficiency of *ADAMTS6* off-target site quantified by amplicon sequencing of DNA extracted from $CFTR^{G542X/G542X}$ intestinal organoid-derived cells transduced with G542X-BE-eVLPs (MOT = ∼60 G542X-BE-eVLPs/cell). Bars represent mean ± SD.

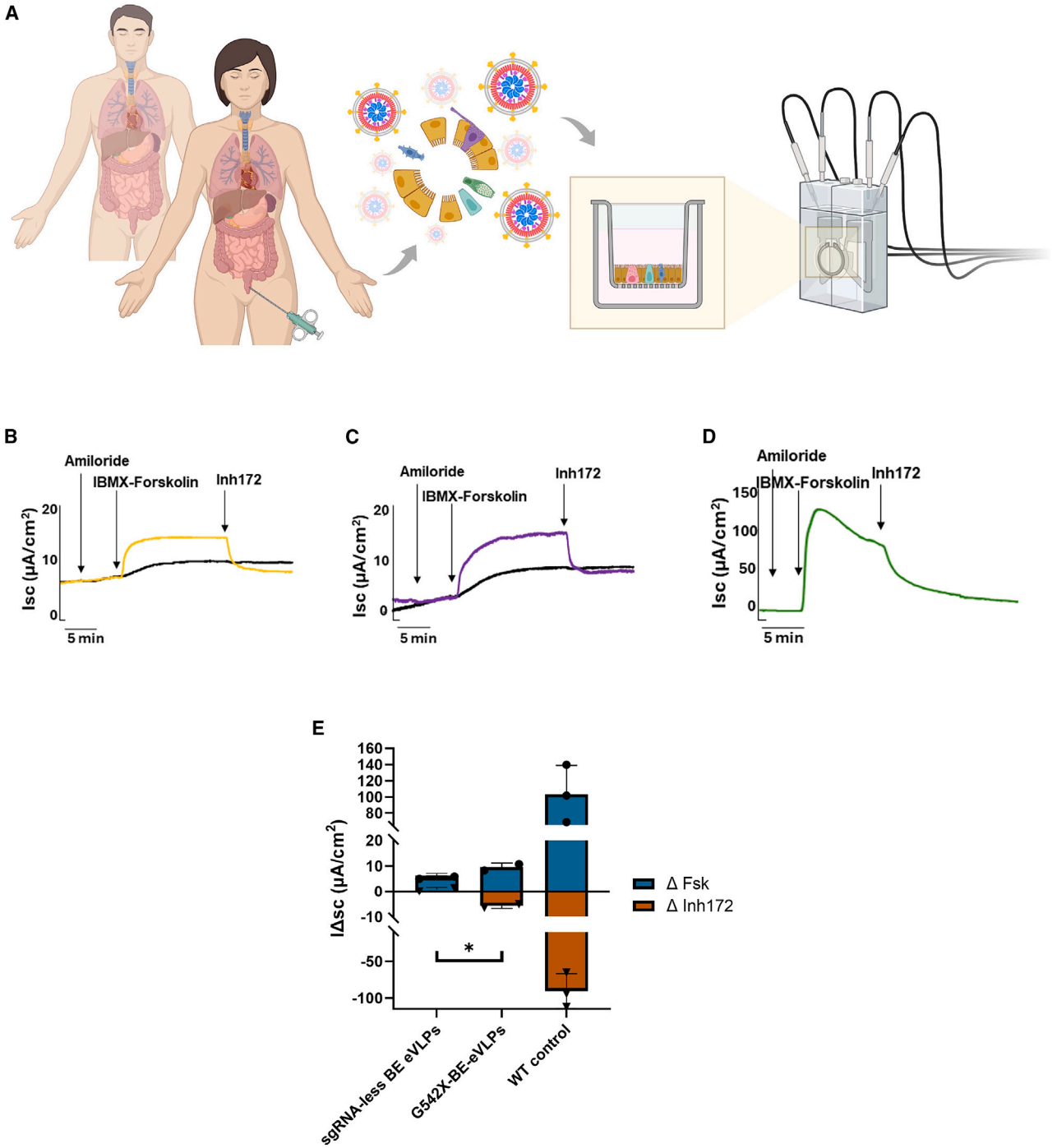

Figure 2. G542R restores CFTR activity in patient-derived intestinal organoids

(A) Graphical abstract of editing strategy and functional study for 2D-grown patient-derived intestinal organoids. Intestinal organoid-derived cells from two *CFTR*$^{G542X/G542X}$ donors were transduced with BE-eVLPs and cultured on filters; CFTR function restoration was quantified with the Ussing chamber assay.

(B and C) Representative tracings of short-circuit current (Isc) measurements of CFTR activity in *CFTR*$^{G542X/G542X}$ intestinal organoid-derived cells from (B) donor #1 and (C) donor #2, transduced with sgRNA-less BE-eVLPs (in black), or with G542X-BE-eVLPs (MOT = ~60 G542X-BE-eVLPs/cells, in yellow or purple).

(D) Representative tracings of short-circuit current (Isc) measurements of CFTR activity in *CFTR*$^{WT/WT}$ intestinal organoid-derived cells.

(E) Response to Fsk (10 μM) and CFTRInh172 (5 μM) of *CFTR*$^{G542X/G542X}$ intestinal organoid-derived cells transduced with sgRNA-less BE-eVLPs (ΔFsk 5.49 ± 0.66 μA/cm^2; ΔInh172 0.77 ± 0.92 μA/cm^2), or with G542X-BE-eVLPs (MOT = ~60 G542X-BE-eVLPs/cell; ΔFsk 9.54 ± 1.70 μA/cm^2; ΔInh172 −5.70 ± 0.97 μA/cm^2), and response of *CFTR*$^{WT/WT}$ intestinal organoid-derived cells (ΔFsk 103.42 ± 35.51 μA/cm^2; ΔInh172 −90.36 ± 23.72 μA/cm^2). Bars represent mean ± SD; *$p \leq 0.05$.

CFTRInh172.[37,38] Response to CFTRInh172 was used as an index of CFTR function. Transduction of *CFTR*$^{G542X/G542X}$ intestinal organoid-derived cells with G542X-BE-eVLPs successfully rescued CFTR activity in both donors (Figures 2B–2D), as evident by the significant response to CFTRInh172 ($p \leq 0.05$; Figure 2E), in contrast to sgRNA-less BE-eVLP-transduced organoids where it was absent (Figures 2B, 2C, and 2E). ~2% editing of G542X to G542R recovered ~6.4% of WT CFTR activity, with negligible variability between the two donors (Figures 2B, 2C, and 2E).

To further validate our approach, we replicated the transduction in *CFTR*$^{G542X/G542X}$ intestinal organoid cells from a third donor and grown in 3D, rather than 2D, for a complementary functional assay (Figure 3A). In 3D organoids grown in Matrigel, cells are oriented such that their apical surface faces inwards; CFTR-mediated Cl^- transport, coupled with water efflux, is directed to the luminal surface and can be quantified as organoid swelling in the Fsk-induced swelling (FIS) assay.[39,40] While Fsk is not CFTR specific, it has been shown that FIS is completely CFTR-dependent.[40] We exploited this assay also to investigate the sensitivity of our system, by testing decreasing BE-eVLP MOTs (~60, ~6, and ~2 G542X-BE-eVLPs/cell). *CFTR*$^{G542X/G542X}$ intestinal organoids mock-transduced with PBS did not exhibit FIS, neither did those transduced with sgRNA-less BE-eVLPs (Figure 3B). Conversely, the *CFTR*$^{G542X/G542X}$ organoids transduced with G542X-BE-eVLPs all displayed FIS, even at a thirtieth of the MOT used in previous experiments (Figures 3B and 3C). The average percentage of FIS-responsive organoids rose with increasing MOTs (1.4%, 4%, and 11.5%, Figure 3C) and reached up to 16% of the total, unsorted population of *CFTR*$^{G542X/G542X}$ organoids transduced with ~60 G542X-BE-eVLPs/cell (Figure 3C). The percentage increase in the area of these FIS-responsive organoids averaged at ~164% at time t = 120′ post stimulation with Fsk (Figure 3D). Their area under the curve (AUC) was significantly higher compared to unrepaired *CFTR*$^{G542X/G542X}$ organoids ($p \leq 0.0001$, Figure 3E) and relative to organoids homozygous for the c.3484C>T mutation (R1162X) transduced with G542X-BE-eVLPs as a negative control ($p \leq 0.0001$, Figures S3C and S3D).

Finally, we investigated whether the newly generated CFTR variant, G542R, might benefit from modulator treatment. We tested the addition of a combination of two correctors and, acutely, a potentiator, Elexacaftor (VX-445), Tezacaftor (VX-661), and Ivacaftor (VX-770), collectively referred to as ETI. ET + I were added in BE-eVLP-edited *CFTR*$^{G542X/G542X}$ organoids grown in 2D or 3D. In both cases, we detected no significant increase in CFTR activity, either measured as ΔIsc or as percentage of swelling organoids, or as AUC, at any of the MOT tested (Figures S2 and S3).

DISCUSSION

The development of modulators provided a highly effective treatment for most people with CF (pwCF); however, correctors and potentiators do not work in pwCF who have two *CFTR* PTC variants, such as G542X, that trigger NMD or generate a severely truncated CFTR protein.[10,41] In the last decade, multiple studies focused on the development of gene editing strategies to correct *CFTR* PTCs and other non-responsive variants.[42] Some of these approaches preferred base editing to precisely repair amenable CF-causing mutations without creating DSBs. Existing base editors, however, could not revert G542X PTC to the WT glycine codon, and only an HDR approach had been reported for this variant to date.[43] Rather, our strategy was to apply adenine base editing to disrupt G542X PTC, thus preventing NMD and restoring the synthesis of full-length CFTR. The G542R variant we generated, albeit not WT, is not listed as CF-causing (www.genet.sickkids.on.ca and www.CFTR2.org) and has been previously shown to retain partial CFTR activity in *in-vitro* models.[23–26] A similar strategy, of installing a non-WT amino acid by adenine base editing, was reported to convert the sickle cell disease β-globin gene *HBB*^{S} to the *HBB*^{G} variant.[44]

We tested our approach in an extensively characterized model of CF, intestinal organoids[27] derived from rectal biopsies of three homozygous *CFTR*$^{G542X/G542X}$ donors. We delivered RNPs of NG-ABE8e and a G542X-specific sgRNA via non-replicating virus-like particles (G542X-BE-eVLPs).[30] Our proposed strategy proved successful in the intestinal organoids derived from all three donors.

In the organoid cells from the first two donors, we attained an average of ~2% editing efficiency, without any selection strategy. The NG-ABE8e editing window enabled the editing of the target nucleotide without modifying any bystander adenines, and the sgRNA we designed did not produce any detectable editing at the top ranking predicted off-target site. The ~2% rescue of G542X PTC resulted in the restoration of CFTR-mediated Cl^- conductance at ~6.4% of WT CFTR levels. The same editing approach in intestinal organoids derived from a third donor recovered the swelling capacity of up to 16% of the total, unsorted population of transduced organoids, with a ~164% increase in organoid area. Improvements in production yields of BE-eVLPs[45] will enable expanded testing to include higher MOTs in the future.

Our data showed a ~3.2-fold amplification of function relative to editing. A recently published study on gene editing for CF applied prime editing to correct a different CF-causing mutation, c.3909C>G (N1303K), and achieved 80% function restoration with 34% editing, a 2.4-fold difference.[46] However, it has been previously demonstrated that Cl^- conductance saturates and can become rate limiting, thus creating a ceiling effect,[47] which could explain the higher fold change achieved at a lower editing efficiency.

The triple combination of Elexacaftor (VX-445), Tezacaftor (VX-661), and Ivacaftor (VX-770) had no additional effect on G542R function in our study. This finding diverges from previous works on G542X readthrough performed in cell lines overexpressing *CFTR*, which showed a G542R response to the corrector Lumacaftor (VX-809)[24] and to the potentiator Ivacaftor (VX-770) alone.[26] Nonetheless, alternative models of CF, with a different *CFTR* expression profile, may respond differently to ETI. Furthermore, it is possible that the concentration of Fsk used in both the short-circuit current and the FIS assays reported in this work saturated CFTR, thus masking any additional effect of ETI. Future research could gain insights from a comparison with airway models and dose-response studies on Fsk to clarify the role of ETI in edited cell.

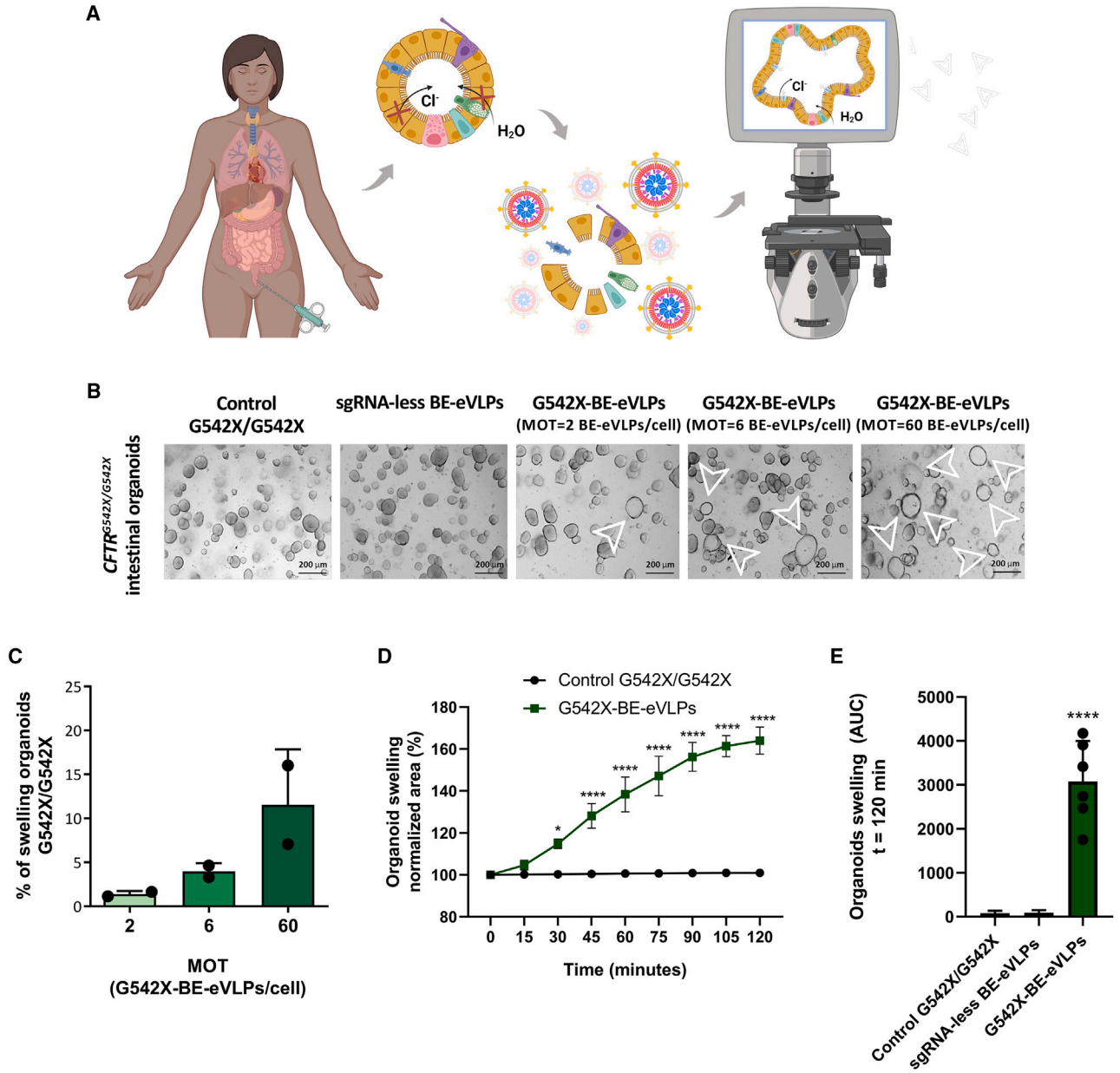

Figure 3. G542X-BE-eVLPs restore FIS in 3D-grown patient-derived intestinal organoids

(A) Graphical abstract of editing strategy and functional study for 3D-grown patient-derived intestinal organoids. Intestinal organoid-derived cells from one *CFTR*$^{G542X/G542X}$ donor were transduced with BE-eVLPs and cultured in Matrigel; CFTR function restoration was assessed in the forskolin-induced swelling (FIS) assay.

(B) Representative bright-field images of *CFTR*$^{G542X/G542X}$ intestinal organoids (scale bars, 200 μm), 120 min post stimulation with forskolin (5 μM). From left to right: organoids mock-transduced with PBS, transduced with sgRNA-less BE-eVLPs, and transduced with increasing concentrations of G542X-BE-eVLPs (MOT = ∼2 G542X-BE-eVLPs/cell, ∼6 G542X-BE-eVLPs/cell, ∼60 G542X-BE-eVLPs/cell). White arrows indicate examples of swelling organoids.

(C) Percentage of swelling organoids, quantified as fraction of FIS-responsive organoids on total *CFTR*$^{G542X/G542X}$ organoids transduced, for each MOT tested. Bars represent mean ± SD.

(D) Percentage increase in *CFTR*$^{G542X/G542X}$ organoids area over time relative to t = 0, following stimulation with forskolin (5 μM). t = 0–120 min; baseline, 100%; mean ± SD; ****$p \leq 0.0001$.

(E) FIS as the absolute area under the curve (AUC) of intestinal organoids *CFTR*$^{G542X/G542X}$ mock-transduced with PBS, transduced with sgRNA-less BE-eVLPs, and transduced with the highest MOT of G542X-BE-eVLPs (∼60 G542X-BE-eVLPs/cell). t = 120 min; baseline, 100%; mean ± SD; ****$p \leq 0.0001$.

A-to-Y base editors (AYBEs) have been developed[48,49] that could potentially edit G542X stop codon (TGA, ACT on the non-coding strand) to the WT glycine (GGA, CCT on the non-coding strand); however, they require a PAM (NGG) that is not available around the G542X mutation. Future studies could benefit from the development of an NG-AYBE with the required editing window to circumvent bystander editing. Additionally, pseudotyping the engineered virus-like particles[50] to target specific cell types of interest could further optimize the delivery strategy, especially for *in-vivo* studies in CF animal models. Prime editing systems could also correct G542X back to WT, though concerns persist regarding the frequency of indel formation and scaffold integration.[51,52]

Our work highlighted the potential of adenine base editing to rescue a severe disease-causing mutation, such as G542X, by installing a non-pathogenic amino acid. We established that significant levels of CFTR function can be achieved even at relatively modest levels of *CFTR* editing and also provided a strategy with the potential for wider applications across multiple diseases.

RESOURCE AVAILABILITY

Lead contact

Further requests may be directed to the lead contact, Patrick T. Harrison (Patrick.Harrison@cchmc.org).

Materials availability

The study did not generate new unique reagents.

Data and code availability

- All the data generated in this study are available from the lead contact upon request.
- This article does not report custom computer code.
- All the software tools used in this study are listed in the key resources table and can be found online.

ACKNOWLEDGMENTS

This study was supported by CF Trust to P.T.H., I.S.-G., and M.F.S. for grant SRC020/ALLEN20XX; CF Foundation to P.T.H. and M.F.S. for grant DRUMM22G0-COLLAB; Fondo per il Programma Nazionale di Ricerca e Progetti di Rilevante Interesse Nazionale (PRIN) to C.S. for grant 2022FRSS2H "Theratyping of Cystic Fibrosis"; and CF Foundation to P.M. for grant Assael08A0. P.T.H. would like to thank Ciaran Lee for helpful discussions and technical advice.

AUTHOR CONTRIBUTIONS

Conceptualization, L.N., M.F.S., and P.T.H.; base editing design, L.N., K.C.-D., and P.T.H.; BE-eVLP production, L.N. and J.B.M.; BE-eVLP qRT-PCR primer design and validation, J.P.C., M.C., L.N., and M.F.S.; BE-eVLP quantification, L.N., L.L., and M.F.S.; base editing experiments and downstream analysis, L.N.; tissue harvesting and biobanking, P.M. and I.S.-G.; tissue culturing, R.V.L., I.P., and E.D.; functional assays, L.N., R.V.L., I.P., and E.D.; data curation and formal analysis, L.N., R.V.L., and I.P.; supervision, M.F.S., P.T.H., P.M., C.S., and I.S.-G.; writing – original draft, L.N.; writing – review and editing, P.M., C.S., I.S.-G., I.P., M.F.S., and P.T.H.; funding acquisition, P.T.H., C.S., and I.S.-G.; resources, P.M., C.S., I.S.-G., M.F.S., and P.T.H.

DECLARATION OF INTERESTS

The authors declare no competing interests.

STAR★METHODS

Detailed methods are provided in the online version of this paper and include the following:

- KEY RESOURCES TABLE
- EXPERIMENTAL MODEL AND STUDY PARTICIPANT DETAILS
  - Biobank establishment and governance
- METHOD DETAILS
  - Culture of intestinal organoids
  - Culture of organoid-derived monolayers
  - Plasmids
  - G542X-BE-eVLP and sgRNA-less BE-eVLP production and purification
  - G542X-BE-eVLP sgRNA extraction and quantification
  - BE-eVLP transduction in organoids
  - Genomic DNA isolation
  - Total RNA isolation and cDNA synthesis
  - Amplicon sequencing and data analysis
  - FIS-assay
  - Ussing chamber assay
- QUANTIFICATION AND STATISTICAL ANALYSIS

SUPPLEMENTAL INFORMATION

Supplemental information can be found online at https://doi.org/10.1016/j.isci.2025.111979.

Received: June 11, 2024
Revised: November 5, 2024
Accepted: February 5, 2025
Published: February 21, 2025

REFERENCES

1. Guo, J., Garratt, A., and Hill, A. (2022). Worldwide rates of diagnosis and effective treatment for cystic fibrosis. J. Cyst. Fibros. *21*, 456–462. https://doi.org/10.1016/j.jcf.2022.01.009.
2. Cutting, G.R. (2015). Cystic fibrosis genetics: From molecular understanding to clinical application. Nat. Rev. Genet. *16*, 45–56. https://doi.org/10.1038/nrg3849.
3. Galietta, L.J.V. (2013). Managing the underlying cause of cystic fibrosis: A future role for potentiators and correctors. Paediatr. Drugs *15*, 393–402. https://doi.org/10.1007/s40272-013-0035-3.
4. Ramsey, B.W., Davies, J., McElvaney, N.G., Tullis, E., Bell, S.C., Dřevínek, P., Griese, M., McKone, E.F., Wainwright, C.E., Konstan, M.W., et al. (2011). A CFTR Potentiator in Patients with Cystic Fibrosis and the G551D Mutation. N. Engl. J. Med. *365*, 1663–1672. https://doi.org/10.1056/nejmoa1105185.
5. Taylor-Cousar, J.L., Munck, A., McKone, E.F., van der Ent, C.K., Moeller, A., Simard, C., Wang, L.T., Ingenito, E.P., McKee, C., Lu, Y., et al. (2017). Tezacaftor–Ivacaftor in Patients with Cystic Fibrosis Homozygous for Phe508del. N. Engl. J. Med. *377*, 2013–2023. https://doi.org/10.1056/nejmoa1709846.
6. Keating, D., Marigowda, G., Burr, L., Daines, C., Mall, M.A., McKone, E.F., Ramsey, B.W., Rowe, S.M., Sass, L.A., Tullis, E., et al. (2018). VX-445–Tezacaftor–Ivacaftor in Patients with Cystic Fibrosis and One or Two Phe508del Alleles. N. Engl. J. Med. *379*, 1612–1620. https://doi.org/10.1056/nejmoa1807120.
7. Heijerman, H.G.M., McKone, E.F., Downey, D.G., Van Braeckel, E., Rowe, S.M., Tullis, E., Mall, M.A., Welter, J.J., Ramsey, B.W., McKee, C.M., et al. (2019). Efficacy and safety of the elexacaftor plus tezacaftor plus ivacaftor combination regimen in people with cystic fibrosis homozygous for the F508del mutation: a double-blind, randomised, phase 3 trial. Lancet *394*, 1940–1948. https://doi.org/10.1016/S0140-6736(19)32597-8.

8. Middleton, P.G., Mall, M.A., Dřevínek, P., Lands, L.C., McKone, E.F., Polineni, D., Ramsey, B.W., Taylor-Cousar, J.L., Tullis, E., Vermeulen, F., et al. (2019). Elexacaftor–Tezacaftor–Ivacaftor for Cystic Fibrosis with a Single Phe508del Allele. N. Engl. J. Med. *381*, 1809–18019. https://doi.org/10.1056/nejmoa1908639.

9. Sharma, J., Keeling, K.M., and Rowe, S.M. (2020). Pharmacological approaches for targeting cystic fibrosis nonsense mutations. Eur. J. Med. Chem. *200*, 112436. https://doi.org/10.1016/j.ejmech.2020.112436.

10. Mutyam, V., Sharma, J., Li, Y., Peng, N., Chen, J., Tang, L.P., Falk Libby, E., Singh, A.K., Conrath, K., and Rowe, S.M. (2021). Novel correctors and potentiators enhance translational readthrough in CFTR nonsense mutations. Am. J. Respir. Cell Mol. Biol. *64*, 604–616. https://doi.org/10.1165/rcmb.2019-0291OC.

11. Aksit, M.A., Bowling, A.D., Evans, T.A., Joynt, A.T., Osorio, D., Patel, S., West, N., Merlo, C., Sosnay, P.R., Cutting, G.R., and Sharma, N. (2019). Decreased mRNA and protein stability of W1282X limits response to modulator therapy. J. Cyst. Fibros. *18*, 606–613. https://doi.org/10.1016/j.jcf.2019.02.009.

12. Sanderlin, E.J., Keenan, M.M., Mense, M., Revenko, A.S., Monia, B.P., Guo, S., and Huang, L. (2022). CFTR mRNAs with nonsense codons are degraded by the SMG6-mediated endonucleolytic decay pathway. Nat. Commun. *13*, 2344. https://doi.org/10.1038/s41467-022-29935-9.

13. Schwank, G., Koo, B.K., Sasselli, V., Dekkers, J.F., Heo, I., Demircan, T., Sasaki, N., Boymans, S., Cuppen, E., van der Ent, C.K., et al. (2013). Functional repair of CFTR by CRISPR/Cas9 in intestinal stem cell organoids of cystic fibrosis patients. Cell Stem Cell *13*, 653–658. https://doi.org/10.1016/j.stem.2013.11.002.

14. Maule, G., Casini, A., Montagna, C., Ramalho, A.S., De Boeck, K., Debyser, Z., Carlon, M.S., Petris, G., and Cereseto, A. (2019). Allele specific repair of splicing mutations in cystic fibrosis through AsCas12a genome editing. Nat. Commun. *10*, 3556. https://doi.org/10.1038/s41467-019-11454-9.

15. Geurts, M.H., de Poel, E., Amatngalim, G.D., Oka, R., Meijers, F.M., Kruisselbrink, E., van Mourik, P., Berkers, G., de Winter-de Groot, K.M., Michel, S., et al. (2020). CRISPR-Based Adenine Editors Correct Nonsense Mutations in a Cystic Fibrosis Organoid Biobank. Cell Stem Cell *26*, 503–510.e7. https://doi.org/10.1016/j.stem.2020.01.019.

16. Li, C., Liu, Z., Anderson, J., Liu, Z., Tang, L., Li, Y., Peng, N., Chen, J., Liu, X., Fu, L., et al. (2023). Prime editing-mediated correction of the CFTR W1282X mutation in iPSCs and derived airway epithelial cells. PLoS One *18*, e0295009. https://doi.org/10.1371/journal.pone.0295009.

17. Anzalone, A.V., Koblan, L.W., and Liu, D.R. (2020). Genome editing with CRISPR–Cas nucleases, base editors, transposases and prime. Nat. Biotechnol. *38*, 824–844. https://doi.org/10.1038/s41587-020-0561-9.

18. Nambiar, T.S., Baudrier, L., Billon, P., and Ciccia, A. (2022). CRISPR-based genome editing through the lens of DNA repair. Mol. Cell *82*, 348–388. https://doi.org/10.1016/j.molcel.2021.12.026.

19. Gaudelli, N.M., Komor, A.C., Rees, H.A., Packer, M.S., Badran, A.H., Bryson, D.I., and Liu, D.R. (2017). Programmable base editing of T to G C in genomic DNA without DNA cleavage. Nature *551*, 464–471. https://doi.org/10.1038/nature24644.

20. Richter, M.F., Zhao, K.T., Eton, E., Lapinaite, A., Newby, G.A., Thuronyi, B.W., Wilson, C., Koblan, L.W., Zeng, J., Bauer, D.E., et al. (2020). Phage-assisted evolution of an adenine base editor with improved Cas domain compatibility and activity. Nat. Biotechnol. *38*, 883–891. https://doi.org/10.1038/s41587-020-0453-z.

21. Mention, K., Cavusoglu-Doran, K., Joynt, A.T., Santos, L., Sanz, D., Eastman, A.C., Merlo, C., Langfelder-Schwind, E., Scallan, M.F., Farinha, C.M., et al. (2023). Use of adenine base editing and homology-independent targeted integration strategies to correct the cystic fibrosis causing variant, W1282X. Hum. Mol. Genet. *32*, 3237–3248. https://doi.org/10.1093/hmg/ddad143.

22. Krishnamurthy, S., Traore, S., Cooney, A.L., Brommel, C.M., Kulhankova, K., Sinn, P.L., Newby, G.A., Liu, D.R., and McCray, P.B. (2021). Functional correction of CFTR mutations in human airway epithelial cells using adenine base editors. Nucleic Acids Res. *49*, 10558–10572. https://doi.org/10.1093/nar/gkab788.

23. Roy, B., Friesen, W.J., Tomizawa, Y., Leszyk, J.D., Zhuo, J., Johnson, B., Dakka, J., Trotta, C.R., Xue, X., Mutyam, V., et al. (2016). Ataluren stimulates ribosomal selection of near-cognate tRNAs to promote nonsense suppression. Proc. Natl. Acad. Sci. USA *113*, 12508–12513. https://doi.org/10.1073/pnas.1605336113.

24. Xue, X., Mutyam, V., Thakerar, A., Mobley, J., Bridges, R.J., Rowe, S.M., Keeling, K.M., and Bedwell, D.M. (2017). Identification of the amino acids inserted during suppression of CFTR nonsense mutations and determination of their functional consequences. Hum. Mol. Genet. *26*, 3116–3129. https://doi.org/10.1093/hmg/ddx196.

25. Fang, X., Yeh, J.T., and Hwang, T.C. (2022). Pharmacological Responses of the G542X-CFTR to CFTR Modulators. Front. Mol. Biosci. *9*, 921680. https://doi.org/10.3389/fmolb.2022.921680.

26. Pranke, I., Bidou, L., Martin, N., Blanchet, S., Hatton, A., Karri, S., Cornu, D., Costes, B., Chevalier, B., Tondelier, D., et al. (2018). Factors influencing readthrough therapy for frequent cystic fibrosis premature termination codons. ERJ Open Res. *4*, 00080-2017. https://doi.org/10.1183/23120541.00080-2017.

27. Van Mourik, P., Beekman, J.M., and Van Der Ent, C.K. (2019). Intestinal organoids to model cystic fibrosis. Eur. Respir. J. *54*, 1802379. https://doi.org/10.1183/13993003.02379-2018.

28. Riesenberg, S., Helmbrecht, N., Kanis, P., Maricic, T., and Pääbo, S. (2022). Improved gRNA secondary structures allow editing of target sites resistant to CRISPR-Cas9 cleavage. Nat. Commun. *13*, 489. https://doi.org/10.1038/s41467-022-28137-7.

29. Chen, B., Gilbert, L.A., Cimini, B.A., Schnitzbauer, J., Zhang, W., Li, G.W., Park, J., Blackburn, E.H., Weissman, J.S., Qi, L.S., and Huang, B. (2013). Dynamic imaging of genomic loci in living human cells by an optimized CRISPR/Cas system. Cell *155*, 1479–1491. https://doi.org/10.1016/j.cell.2013.12.001.

30. Banskota, S., Raguram, A., Suh, S., Du, S.W., Davis, J.R., Choi, E.H., Wang, X., Nielsen, S.C., Newby, G.A., Randolph, P.B., et al. (2022). Engineered virus-like particles for efficient *in vivo* delivery of therapeutic proteins. Cell *185*, 250–265.e16. https://doi.org/10.1016/j.cell.2021.12.021.

31. Clement, K., Rees, H., Canver, M.C., Gehrke, J.M., Farouni, R., Hsu, J.Y., Cole, M.A., Liu, D.R., Joung, J.K., Bauer, D.E., and Pinello, L. (2019). CRISPResso2 provides accurate and rapid genome editing sequence analysis. Nat. Biotechnol. *37*, 224–226. https://doi.org/10.1038/s41587-019-0032-3.

32. Rees, H.A., and Liu, D.R. (2018). Base editing: precision chemistry on the genome and transcriptome of living cells. Nat. Rev. Genet. *19*, 770–788. https://doi.org/10.1038/s41576-018-0059-1.

33. Hsu, P.D., Scott, D.A., Weinstein, J.A., Ran, F.A., Konermann, S., Agarwala, V., Li, Y., Fine, E.J., Wu, X., Shalem, O., et al. (2013). DNA targeting specificity of RNA-guided Cas9 nucleases. Nat. Biotechnol. *31*, 827–832. https://doi.org/10.1038/nbt.2647.

34. Concordet, J.P., and Haeussler, M. (2018). CRISPOR: Intuitive guide selection for CRISPR/Cas9 genome editing experiments and screens. Nucleic Acids Res. *46*, W242–W245. https://doi.org/10.1093/nar/gky354.

35. Rabinowitz, R., and Offen, D. (2021). Single-Base Resolution: Increasing the Specificity of the CRISPR-Cas System in Gene Editing. Mol. Ther. *29*, 937–948. https://doi.org/10.1016/j.ymthe.2020.11.009.

36. Birimberg-Schwartz, L., Ip, W., Bartlett, C., Avolio, J., Vonk, A.M., Gunawardena, T., Du, K., Esmaeili, M., Beekman, J.M., Rommens, J., et al. (2023). Validating organoid-derived human intestinal monolayers for personalized therapy in cystic fibrosis. Life Sci. Alliance *6*, e202201857. https://doi.org/10.26508/lsa.202201857.

37. Ramalho, A.S., Boon, M., Proesmans, M., Vermeulen, F., Carlon, M.S., and Boeck, K.D. (2022). Assays of CFTR Function In Vitro, Ex Vivo and In Vivo. Int. J. Mol. Sci. *23*, 1437. https://doi.org/10.3390/ijms23031437.

38. Li, H., Sheppard, D.N., and Hug, M.J. (2004). Transepithelial electrical measurements with the Ussing chamber. J. Cyst. Fibros. *3*, 123–126. https://doi.org/10.1016/j.jcf.2004.05.026.

39. Boj, S.F., Vonk, A.M., Statia, M., Su, J., Vries, R.R.G., Beekman, J.M., and Clevers, H. (2017). Forskolin-induced swelling in intestinal organoids: An *in vitro* assay for assessing drug response in cystic fibrosis patients. J. Vis. Exp. *2017*, 55159. https://doi.org/10.3791/55159.

40. Dekkers, J.F., Wiegerinck, C.L., De Jonge, H.R., Bronsveld, I., Janssens, H.M., de Winter-de Groot, K.M., Brandsma, A.M., de Jong, N.W.M., Bijvelds, M.J.C., Scholte, B.J., et al. (2013). A functional CFTR assay using primary cystic fibrosis intestinal organoids. Nat. Med. *19*, 939–945. https://doi.org/10.1038/nm.3201.

41. Haggie, P.M., Phuan, P.W., Tan, J.A., Xu, H., Avramescu, R.G., Perdomo, D., Zlock, L., Nielson, D.W., Finkbeiner, W.E., Lukacs, G.L., and Verkman, A.S. (2017). Correctors and potentiators rescue function of the truncated W1282X-Cystic Fibrosis Transmembrane Regulator (CFTR) translation product. J. Biol. Chem. *292*, 771–785. https://doi.org/10.1074/jbc.M116.764720.

42. Bulcaen, M., and Carlon, M.S. (2024). Genetic surgery for a cystic fibrosis-causing splicing mutation. Mol. Ther. Methods Clin. Dev. *32*, 101177. https://doi.org/10.1016/j.omtm.2023.101177.

43. Wei, T., Sun, Y., Cheng, Q., Chatterjee, S., Traylor, Z., Johnson, L.T., Coquelin, M.L., Wang, J., Torres, M.J., Lian, X., et al. (2023). Lung SORT LNPs enable precise homology-directed repair mediated CRISPR/Cas genome correction in cystic fibrosis models. Nat. Commun. *14*, 7322. https://doi.org/10.1038/s41467-023-42948-2.

44. Newby, G.A., Yen, J.S., Woodard, K.J., Mayuranathan, T., Lazzarotto, C.R., Li, Y., Sheppard-Tillman, H., Porter, S.N., Yao, Y., Mayberry, K., et al. (2021). Base editing of haematopoietic stem cells rescues sickle cell disease in mice. Nature *595*, 295–302. https://doi.org/10.1038/s41586-021-03609-w.

45. Raguram, A., An, M., Chen, P.Z., and Liu, D.R. (2024). Directed evolution of engineered virus-like particles with improved production and transduction efficiencies. Nat. Biotechnol. 1–13. https://doi.org/10.1038/s41587-024-02467-x.

46. Bulcaen, M., Kortleven, P., Liu, R.B., Maule, G., Dreano, E., Kelly, M., Ensinck, M.M., Thierie, S., Smits, M., Ciciani, M., et al. (2024). Prime editing functionally corrects cystic fibrosis-causing CFTR mutations in human organoids and airway epithelial cells. Cell Rep. Med. *5*, 101544. https://doi.org/10.1016/j.xcrm.2024.101544.

47. Johnson, L.G., Olsen, J.C., Sarkadi, B., Moore, K.L., Swanstrom, R., and Boucher, R.C. (1992). Efficiency of gene transfer for restoration of normal airway epithelial function in cystic fibrosis. Nat. Genet. *2*, 21–25. https://doi.org/10.1038/ng0992-21.

48. Chen, L., Hong, M., Luan, C., Gao, H., Ru, G., Guo, X., Zhang, D., Zhang, S., Li, C., Wu, J., et al. (2024). Adenine transversion editors enable precise, efficient A●T-to-C●G base editing in mammalian cells and embryos. Nat. Biotechnol. *42*, 638–650. https://doi.org/10.1038/s41587-023-01821-9.

49. Tong, H., Wang, X., Liu, Y., Liu, N., Li, Y., Luo, J., Ma, Q., Wu, D., Li, J., Xu, C., and Yang, H. (2023). Programmable A-to-Y base editing by fusing an adenine base editor with an N-methylpurine DNA glycosylase. Nat. Biotechnol. *41*, 1080–1084. https://doi.org/10.1038/s41587-022-01595-6.

50. Hamilton, J.R., Chen, E., Perez, B.S., Sandoval Espinoza, C.R., Kang, M.H., Trinidad, M., Ngo, W., and Doudna, J.A. (2024). In vivo human T cell engineering with enveloped delivery vehicles. Nat. Biotechnol. *42*, 1684–1692. https://doi.org/10.1038/s41587-023-02085-z.

51. Anzalone, A.V., Randolph, P.B., Davis, J.R., Sousa, A.A., Koblan, L.W., Levy, J.M., Chen, P.J., Wilson, C., Newby, G.A., Raguram, A., and Liu, D.R. (2019). Search-and-replace genome editing without double-strand breaks or donor DNA. Nature *576*, 149–157. https://doi.org/10.1038/s41586-019-1711-4.

52. Koeppel, J., Weller, J., Peets, E.M., Pallaseni, A., Kuzmin, I., Raudvere, U., Peterson, H., Liberante, F.G., and Parts, L. (2023). Prediction of prime editing insertion efficiencies using sequence features and DNA repair determinants. Nat. Biotechnol. *41*, 1446–1456. https://doi.org/10.1038/s41587-023-01678-y.

53. Felício, V., Ramalho, A.S., Igreja, S., and Amaral, M.D. (2017). mRNA-based detection of rare CFTR mutations improves genetic diagnosis of cystic fibrosis in populations with high genetic heterogeneity. Clin. Genet. *91*, 476–481. https://doi.org/10.1111/cge.12802.

54. Schindelin, J., Arganda-Carreras, I., Frise, E., Kaynig, V., Longair, M., Pietzsch, T., Preibisch, S., Rueden, C., Saalfeld, S., Schmid, B., et al. (2012). Fiji: An open-source platform for biological-image analysis. Nat. Methods *9*, 676–682. https://doi.org/10.1038/nmeth.2019.

55. Kleinfelder, K., Somenza, E., Farinazzo, A., Conti, J., Lotti, V., Latorre, R.V., Rodella, L., Massella, A., Tomba, F., Bertini, M., et al. (2023). CFTR Modulators Rescue the Activity of CFTR in Colonoids Expressing the Complex Allele p.[R74W;V201M;D1270N]/dele22_24. Int. J. Mol. Sci. *24*, 5199. https://doi.org/10.3390/ijms24065199.

56. Kleinfelder, K., Villella, V.R., Hristodor, A.M., Laudanna, C., Castaldo, G., Amato, F., Melotti, P., and Sorio, C. (2023). Theratyping of the Rare CFTR Genotype A559T in Rectal Organoids and Nasal Cells Reveals a Relevant Response to Elexacaftor (VX-445) and Tezacaftor (VX-661) Combination. Int. J. Mol. Sci. *24*, 10358. https://doi.org/10.3390/ijms241210358.

57. Dreano, E., Burgel, P.R., Hatton, A., Bouazza, N., Chevalier, B., Macey, J., Leroy, S., Durieu, I., Weiss, L., Grenet, D., et al. (2023). Theratyping cystic fibrosis patients to guide elexacaftor/tezacaftor/ivacaftor out-of-label prescription. Eur. Respir. J. *62*, 2300110. https://doi.org/10.1183/13993003.00110-2023.

STAR★METHODS

KEY RESOURCES TABLE

REAGENT or RESOURCE	SOURCE	IDENTIFIER
Bacterial and virus strains		
NEB® 5-alpha chemically competent E. coli	NEB	Cat#C2987H
Biological samples		
Patient-derived intestinal organoids	Institut Necker Enfants Malades, Paris, France Azienda Ospedaliera di Verona, Verona, Italy	N/A
Chemicals, peptides, and recombinant proteins		
DMEM/F12	Gibco	Cat#11580546
Glutamax	Gibco	Cat#35050061
Y-27632	Selleck Chemicals	Cat#S6390
A83-01	Tocris	Cat#2939
SB431542	Tocris	Cat#1614
SB202190	Sigma	Cat#S7067
GSK3 inhibitor	Stemcell Technologies	Cat#72054
Matrigel	Corning	Cat#356255
TrypLE	Thermo Fisher	Cat#12605010
jetPRIME transfection reagent	Polyplus	Cat#101000001
PEG-it Virus Precipitation Solution	System Biosciences	Cat#LV825A-1
Forskolin	Sigma	Cat#F3917
Critical commercial assays		
QIAmp Viral RNA Mini Kit	QIAGEN	Cat#52904
DNeasy Blood & Tissue Kit	QIAGEN	Cat#69504
Monarch® Total RNA Miniprep Kit	NEB	Cat#T2010S
PlasmidPlus Midi Kit	QIAGEN	Cat#12941
PlasmidPlus Maxi Kit	QIAGEN	Cat#12963
LunaScript RT SuperMix Kit	NEB	Cat#E3010S
LightCycler® 480 SYBR Green I Master	Roche	Cat#04707516001
Q5® High-Fidelity 2X Master Mix	NEB	Cat#M0492L
Experimental models: Cell lines		
Gesicle Producer 293T cells	Takara Bio	Cat#632617
Oligonucleotides		
sgRNA G542X: ACCTTCTCAAAGAACTATATGT TTAAGAGCTATGCTGGAAACAG CATAGCAAGTTTAAATAAGGCT AGTCCGTTATCAACTTGAAAAA GTGGCACCGAGTCGGTGCTTTTTTT	IDT	custom designed
Primers qPCR BE-eVLPs fw/rv: TGCTGGAAACAGCATAGCAAGTTT / GACTCGGTGCCACTTTTTCAAGTT	Eurofins Genomics	custom designed

(*Continued on next page*)

Continued

REAGENT or RESOURCE	SOURCE	IDENTIFIER
Primers amplification *CFTR* exon 12 with illumina adapters, fw/rv: ACACTCTTTCCCTACACGACGC TCTTCCGATCTGAAGGAAGATGTGCCTTTCA / GACTGGAGTTCAGACGTGTGCT CTTCCGATCTGGCACAGATTCTGAGTAACC	Eurofins Genomics	custom designed
Primers amplification *CFTR* exon 12 cDNA fw/rv: GGCACCATTAAAGAAAATATCATCTT / CAAATCAGCATCTTTGTATACTG	Eurofins Genomics	Ramalho et al.[53]
Primers amplification *ADAMTS6* off-target site fw/rv: TTCCTGACCAAGGCTGCTTA / ATCCAGCAAACTAGCATACCA	Eurofins Genomics	custom designed
Recombinant plasmid DNA		
pCMV-MMLVgag-3xNES-ABE8e-NG	Addgene	Cat#181754
pBS-CMV-gagpol	Addgene	Cat#35614
pCMV-VSV-G	Addgene	Cat#8454
pU6-G542X-sgRNA-HEAT	IDT	custom designed
Software and algorithms		
Image J	Schindelin et al.[54]	https://imagej.net/software/fiji/#publication
GraphPad Prism version 10	GraphPad Software, Boston, Massachusetts USA	https://www.graphpad.com/features
CRISPOR	Concordet et al.[34]	http://crispor.tefor.net/
CRISPResso2	Clement et al.[31]	http://crispresso2.pinellolab.org/submission
Geneious Prime	N/A	https://www.geneious.com
Biorender	N/A	https://www.biorender.com/

EXPERIMENTAL MODEL AND STUDY PARTICIPANT DETAILS

Biobank establishment and governance

Primary cells were obtained from rectal biopsies of six donors (3 with CF and 3 non-CF). Information related to age, gender, ancestry or ethnicity is not disclosed.

Collection of intestinal organoids in Italy followed the guidelines of the Declaration of Helsinki and was approved by the Institutional Review Board CRCFC-CFTR050. Informed consent was obtained before colonoscopy examination from the subjects involved in the study. The whole procedure regarding organoid culture and analysis, that includes standard protocols for specimen collection and storage, theratyping, functional analysis and data elaboration, is described in detail in recent publications.[55,56] All experimentation performed in France using human tissue was approved by the Ile de France 2 Ethics Committee CPP IDF2: 2010-05-03-3. Written, informed consent, for tissue collection and generation of organoids, was obtained from each adult and parent. All experiments were performed in accordance with the guidelines and regulations described by the Declaration of Helsinki and the low Huriet-Serusclat on human research ethics.

Culture conditions are described in the method details section.

METHOD DETAILS

Culture of intestinal organoids

Intestinal organoids were obtained from rectal biopsies. Briefly, biopsies were recovered in a surgical medium (DMEM/F12 medium, Gibco, Cat#11580546) with antibiotics (50 μg/mL gentamicin, 50 μg/mL vancomycin) and an antifungal (2.5 μg/mL amphotericin B). They were then incubated in 10 mM EDTA for 90–120 minutes at 4°C. Isolated crypts were washed with a cold PBS solution, resuspended in 50% Matrigel (3D matrix, Corning, Cat#356255), and seeded in 24-well culture plates at a density of 50–100 crypts/well in 40 μL of Matrigel. Following Matrigel polymerization, crypts were cultured in pre-warmed complete medium: advanced DMEM/F12 supplemented with 1% penicillin and streptomycin, 0.2% primocin, 10 mM HEPES, 1% Glutamax (Gibco, Cat#35050061), 1X N2, 1X B27, 1.25 mM N-acetylcysteine, 50 ng/mL mouse epidermal growth factor (mEGF), 50% Wnt3a-conditioned medium (WCM), 10% noggin-conditioned medium (NCM), 20% Rspo1-conditioned medium, 10 mM nicotinamide, 10 nM gastrin, 500 nM A83-01 (Tocris, Cat#2939), 1 μM SB431542 (Tocris, Cat#1614), 10 nM PGE and 3 μM SB202190 (Sigma, Cat#S7067). The complete medium was further supplemented during the first week of cell culture with 10 μM Rho inhibitor Y-27623 (Selleck Chemicals, Cat#S6390),

10 μM GSK3 inhibitor CHIR-99021 (Stemcell Technologies, Cat#72054), 50 μg/mL gentamicin, 50 μg/mL vancomycin and 2.5 μg/mL amphotericin B. The medium was then refreshed every 2–3 days and the outgrowing crypts/organoids were expanded every 7–10 days.

Culture of organoid-derived monolayers

Organoid-derived monolayers were cultured on type IV collagen-coated porous filters with a 0.33-cm^2 surface (Transwell, Corning,Cat#CLS3401-48EA). 7-day old organoid cultures were trypsinized with TrypLE (Thermo Fisher, Cat#12605010) at 37°C and mechanically disrupted after incubation. 2.5x10^5 organoid-derived cells were seeded per insert, with the addition of 100 μL and 600 μL of organoid growth medium supplemented with Y-27632 (10 μM), at the apical and basolateral sides respectively. Organoid growth medium was refreshed every 2-3 days. Electrophysiological measurements were performed after 21 days of growth and differentiation in liquid-liquid interface (LLI) conditions (described in detail by[57]).

Plasmids

Plasmids used in this study include: pCMV-MMLVgag-3xNES-ABE8e-NG (Addgene plasmid #181754), a kind gift from David Liu; pBS-CMV-gagpol (Addgene plasmid #35614), a kind gift from Patrick Salmon; pCMV-VSV-G (Addgene plasmid #8454), a kind gift from Bob Weinberg; pU6-G542X-sgRNA-HEAT, custom-designed and purchased from Integrated DNA Technologies (IDT). All the plasmids in this study were propagated in NEB® 5-alpha chemically competent E. coli (New England Biolabs, NEB, Cat#C2987H) and purified for transfection using a PlasmidPlus Midi Kit (QIAGEN, Cat#12941) or PlasmidPlus Maxi Kit (QIAGEN, Cat#12963) with endotoxin removal. Plasmid identity was confirmed by Sanger Sequencing (Eurofins Genomics) and pair-wise alignment on Geneious Prime software platform.

G542X-BE-eVLP and sgRNA-less BE-eVLP production and purification

G542X-BE-eVLPs and sgRNA-less BE-eVLPs used in this study were version v4, produced as described by Banskota and colleagues.[30] In brief, the vectors were produced by transient transfection of Gesicle Producer 293T cells (Takara Bio, Cat#632617) by jetPRIME transfection reagent (Polyplus, Cat#101000001) according to the manufacturer's instructions. For the production of G542X-BE-eVLPs, we co-transfected pCMV-MMLVgag-3xNES-ABE8e-NG, pBS-CMV-gagpol, pCMV-VSV-G and pU6-G542XsgRNA-HEAT. For sgRNA-less BE-eVLPs we co-transfected pCMV-MMLVgag-3xNES-ABE8e-NG, pBS-CMV-gagpol and pCMV-VSV-G only. 48 h post-transfection, Gesicle cell supernatant was harvested and centrifuged for 5 min at 500 x g to remove cell debris. The clarified supernatant was filtered through a 0.45-μm PVDF filter and concentrated 300-fold using PEG-it Virus Precipitation Solution (System Biosciences, Cat#LV825A-1) according to the manufacturer's protocol. G542X-BE-eVLPs and sgRNA-less BE-eVLPs were recovered as a pellet by centrifugation for 30 min at 1500 x g and 4°C and resuspended in the appropriate volume of cold PBS for the concentration required. The 300X-concentrated BE-eVLP preps were then diluted 3-fold in PBS (100X) or concentrated 10-fold (3000X) by a further round of centrifugation at 1500 x g (30 min at 4°C); this step was deemed necessary to test different MOTs of BE-eVLPs within the limited volume capacity allowed by the 2D and 3D culture of intestinal organoids, respectively on filters and in Matrigel.

G542X-BE-eVLP sgRNA extraction and quantification

G542X-BE-eVLP RNA was extracted using the QIAmp Viral RNA Mini Kit (QIAGEN, Cat#52904) according to the manufacturer's instructions, and treated with DNase I to remove any DNA carry-over. Extracted RNA was reverse transcribed using LunaScript RT SuperMix Kit (NEB, Cat#E3010S) according to the manufacturer's protocols. qPCR was performed on sgRNA cDNA using the LightCycler 480_1536 Real-Time PCR Detection System (Roche) with LightCycler® 480 SYBR Green I Master (Roche, Cat#04707516001), and the following primers:

Primer name	Primer sequence 5' - 3'
qPCR_BE-eVLPs_fw	TGCTGGAAACAGCATAGCAAGTTT
qPCR_BE-eVLPs_rv	GACTCGGTGCCACTTTTTCAAGTT

A chemically synthesized DNA oligo (IDT) of the sgRNA cDNA sequence was used for standard curve generation. The multiplicities of transduction (MOTs) used in this study were defined as the number of G542X-BE-eVLPs per cell. MOTs were estimated by calculating the sgRNA copy number per μl of G542X-BE-eVLP prep and assuming an average of 50 RNPs/BE-eVLP, as reported by.[30]

The RT-qPCR-based quantification of the G542X-BE-eVLPs used in this study was estimated on the 300X-concentrated prep, that was applied to patient-derived intestinal organoids at an MOT = ∼6 G542X-BE-eVLPs/cell, and was diluted 3-fold (MOT = ∼2 G542X-BE-eVLPs/cell) or concentrated 10-fold (MOT = ∼60 G542X-BE-eVLPs/cell). The sgRNA-less BE-eVLPs, on which the RT-qPCR could not be performed, were prepared and handled identically and in parallel to G542X-BE-eVLPs.

BE-eVLP transduction in organoids

On the day of transduction, intestinal organoids were dissociated into single cells using TrypLE solution (Thermo Fisher Scientific, Cat#12605010) for 10 minutes at 37°C. After dissociation, organoid-derived single cells were counted and centrifuged at 500 x g for 5 minutes. Pelleted cells were resuspended in sgRNA-less BE-eVLPs or G542X-BE-eVLPs at three MOTs (~2, ~6 and ~60 G542X-BE-eVLPs/cell), or mock-transduced with PBS, and incubated at 37°C for 15 minutes in a water bath. Following transduction in suspension, for every condition, the organoid-derived transduced cells were mixed with 50% Matrigel and plated out as a single 5 μL droplet per well on 96-well tissue culture plates. Following polymerization, Matrigel droplets were covered in 50 μL of complete culture medium. Newly developing organoids were maintained at 37°C and 5% CO_2 for 7 days before Forskolin Induced Swelling (FIS) assays were performed. Transduced organoid-derived cells destined for the Ussing Chamber Assay, instead, were seeded on 0.33-cm^2-surface filters, where they were grown and maintained in LLI at 37°C and 5% CO_2 for 21 days before the assay.

Genomic DNA isolation

Genomic DNA from organoid-derived cells was harvested from 0.33 cm^2-surface filters by scraping. DNA was extracted using the DNeasy Blood & Tissue Kit (QIAGEN, Cat#69504) according to manufacturer's protocols.

Total RNA isolation and cDNA synthesis

RNA from organoid-derived cells was harvested from 0.33 cm^2-surface filters by scraping. RNA was extracted using the Monarch® Total RNA Miniprep Kit (NEB, Cat#T2010S) according to manufacturer's protocols. Extracted RNA was reverse transcribed using LunaScript RT SuperMix Kit (NEB, Cat#E3010S) according to the manufacturer's protocols.

Amplicon sequencing and data analysis

Target regions of DNA and cDNA from organoid-derived cells were amplified using Q5® High-Fidelity 2X Master Mix (NEB, Cat#M0492L). Amplicon sequencing was performed by GENEWIZ (Azenta Life Sciences). FASTQ files were analyzed using CRISPResso2, to quantify ABE-mediated genomic alterations, indels, bystanders and off-target. *In-silico* prediction of off-targets was performed with CRISPOR.

Application	Primer name	Primer sequence 5'-3'
Amplicon-sequencing of *CFTR* exon 12	*CFTR*in11_fw_ill	ACACTCTTTCCCTACACGACGCTCTT CCGATCTGAAGGAAGATGTGCCTTTCA
Amplicon-sequencing of *CFTR* exon 12	*CFTR*in12_rv_ill	GACTGGAGTTCAGACGTGTGCTCTTC CGATCTGGCACAGATTCTGAGTAACC
Amplicon-sequencing of *CFTR* exon 12 cDNA	CF10N[53]	GGCACCATTAAAGAAAATATCATCTT
Amplicon-sequencing of *CFTR* exon 12 cDNA	561AL[53]	CAAATCAGCATCTTTGTATACTG
Amplicon-sequencing of *ADAMTS6* off-target site	*ADAMTS6*in17_fw	TTCCTGACCAAGGCTGCTTA
Amplicon-sequencing of *ADAMTS6* off-target site	*ADAMTS6*in18_rv	ATCCAGCAAACTAGCATACCA

FIS-assay

Transduced rectal organoids were seeded in a 96-well culture plate 7 days prior to FIS (see BE-eVLP transduction in organoids) and were treated with DMSO or a combination of CFTR correctors (VX-661 and VX-445, 3 μM) for 24 h. Immediately before FIS, samples were stimulated acutely with CFTR agonist Forskolin (5 μM) ± the enhancer VX-770 (3 μM) in specific conditions, and analyzed by EVOS microscopy with a 4X objective in a controlled atmosphere 37°C, 20% O_2 and 5% CO_2 (EVOS Cell Imaging System with onstage incubator, Thermo Fisher Scientific). Images were acquired every 15 minutes for a total of 120 minutes in time lapse video. The increase in total area (xy plane) relative to t = 0 of Forskolin treatment was calculated using Image J software (Fiji) and normalized to the initial area. The normalized data are expressed as total area under the curve (AUC, t= 120 min, baseline, 100%), calculated using GraphPad Prism software.

Ussing chamber assay

Short-circuit-current (Isc) was measured under voltage clamp conditions with an EVC4000 Precision V/I Clamp (World Precision Instruments). Chloride gradient across the epithelium was created by differential composition of basal and apical Ringer solutions. The basal Ringer solution contained: 145 mM NaCl, 3.3 mM K_2HPO_4, 10 mM HEPES, 10 mM D-Glucose, 1.2 mM $MgCl_2$, and 1.2 mM $CaCl_2$. The apical solution contained: 145 mM Na-Gluconate, 3.3 mM K_2HPO_4, 10 mM HEPES, 10 mM D-Glucose, 1.2 mM $MgCl_2$, 1.2 mM $CaCl_2$. Inhibitors and activators were added after stabilization of baseline Isc: sodium channel blocker Amiloride (100 μM); cAMP agonist Forskolin (10 μM) and 3-isobutyl-1-methylxanthine (IBMX 100 μM) to activate the transepithelial cAMP-dependent current (including Cl^- transport through CFTR channels); VX-770 (10 μM) to potentiate CFTR activity; CFTR inhibitor

CFTRInh172 (5 μM) to specifically inhibit CFTR; and ATP (100 μM) to challenge the purinergic calcium-dependent Cl^- secretion. The change of Isc (ΔIsc) upon CFTRInh172 application served as an index of CFTR function. In specific conditions, organoid-derived cells were incubated with VX-445 and VX-661 (3 μM each) for 48h before Isc measurements, and VX-770 (10 μM) was added acutely to the Ussing chambers during the experiment.

QUANTIFICATION AND STATISTICAL ANALYSIS

Data are shown as mean and standard deviation (SD). No statistical methods were used to predetermine sample size. Statistical analysis was performed using GraphPad Prism software. Sample size and p-values are described in the figure legends. Statistical tests used include unpaired t-test for % of swelling organoids, ordinary one-way ANOVA for organoids swelling (AUC), two-way ANOVA for organoids swelling over time, paired t-test for organoids swelling with or without ETI, multiple t-tests for Isc measurements.